Title
Characteristics of the atmospheric CO2 signal as observed over the conterminous United States during INTEX-NA

Journal
Journal of Geophysical Research, 113(D7)

ISSN
0148-0227

Authors
Choi, Yonghoon
Vay, Stephanie A
Vadrevu, Krishna P
et al.

Publication Date
2008

DOI
10.1029/2007jd008899

Characteristics of the atmospheric CO_2 signal as observed over the conterminous United States during INTEX-NA

Yonghoon Choi,[1] Stephanie A. Vay,[2] Krishna P. Vadrevu,[3] Amber J. Soja,[1] Jung-Hun Woo,[4] Scott R. Nolf,[5] Glen W. Sachse,[2] Glenn S. Diskin,[2] Donald R. Blake,[6] Nicola J. Blake,[6] Hanwant B. Singh,[7] Melody A. Avery,[2] Alan Fried,[8] Leonhard Pfister,[7] and Henry E. Fuelberg[9]

Received 27 April 2007; revised 2 November 2007; accepted 12 December 2007; published 1 April 2008.

[1] High resolution in situ measurements of atmospheric CO_2 were made from the NASA DC-8 aircraft during the Intercontinental Chemical Transport Experiment–North America (INTEX-NA) campaign, part of the wider International Consortium for Atmospheric Research on Transport and Transformation (ICARTT). During the summer of 2004, eighteen flights comprising 160 h of measurements were conducted within a region bounded by 27 to 53°N and 36 to 139°W over an altitude range of 0.15 to 12 km. These large-scale surveys provided the opportunity to examine the characteristics of the atmospheric CO_2 signal over sparsely sampled areas of North America and adjacent ocean basins. The observations showed a high degree of variability ($\leq$18%) due to the myriad source and sink processes influencing the air masses intercepted over the INTEX-NA sampling domain. Surface fluxes had strong effects on continental scale concentration gradients. Clear signatures of CO_2 uptake were seen east of the Mississippi River, notably a persistent CO_2 deficit in the lowest 2–3 km. When combining the airborne CO_2 measurements with LANDSAT and MODIS data products, the lowest CO_2 mixing ratios observed during the campaign (337 ppm) were tied to mid-continental agricultural fields planted in corn and soybeans. We used simultaneous measurements of CO, O_3, C_2Cl_4, C_2H_6, C_2H_2 and other unique chemical tracers to differentiate air mass types. Coupling these distinct air mass chemical signatures with transport history permitted identification of convection, stratosphere-troposphere exchange, long-range transport from Eastern Asia, boreal wildfires, and continental outflow as competing processes at multiple scales influencing the observed concentrations. Our results suggest these are important factors contributing to the large-scale distribution in CO_2 mixing ratios thus these observations offer new constraints in the computation of the North American carbon budget.

Citation: Choi, Y., et al. (2008), Characteristics of the atmospheric CO_2 signal as observed over the conterminous United States during INTEX-NA, *J. Geophys. Res.*, *113*, D07301, doi:10.1029/2007JD008899.

1. Introduction

[2] Within the short span of six years since the United Nations IPCC Third Assessment Report, the influence of human activities on climate has become more discernable. The increase in anthropogenic greenhouse gas concentrations, notably CO_2, is now very likely contributing to the higher globally averaged temperatures recorded since the mid-20th century [*IPCC*, 2007]. Carbon dioxide has increased in the atmosphere since the pre-industrial period (280 ppm) [*IPCC*, 2001] and emitted CO_2 has been distributed into the atmosphere, oceans, and terrestrial biosphere which serve as active CO_2 reservoirs. In 2005, the global mean CO_2 mixing ratio reached its highest level in the past 650,000 years [*Siegenthaler et al.*, 2005] at 379 ppm following an annual mean growth rate of 1.9 ppm yr^{-1} during the last ten years (1995–2005) [*IPCC*, 2007]. This high mixing ratio suggests strong net sources in the northern high and midlatitudes due primarily to the combustion of fossil fuels and land use change. The Environmental Protection Agency (EPA) carbon inventory report [*EPA*, 2006] shows that the total U.S. greenhouse gas emissions were

[1]National Institute of Aerospace, Hampton, Virginia, USA.
[2]NASA Langley Research Center, Hampton, Virginia, USA.
[3]Agroecosystem Management Program, Ohio Agricultural Research and Development Center (OARDC), The Ohio State University, Wooster, Ohio, USA.
[4]Department of Advanced Technology Fusion, Konkuk University, Seoul, Korea.
[5]Computer Sciences Corporation, Hampton, Virginia, USA.
[6]Department of Chemistry, University of California, Irvine, California, USA.
[7]NASA Ames Research Center, Moffett Field, California, USA.
[8]National Center for Atmospheric Research, Boulder, Colorado, USA.
[9]Department of Meteorology, Florida State University, Tallahassee, Florida, USA.

0148-0227/08/2007JD008899

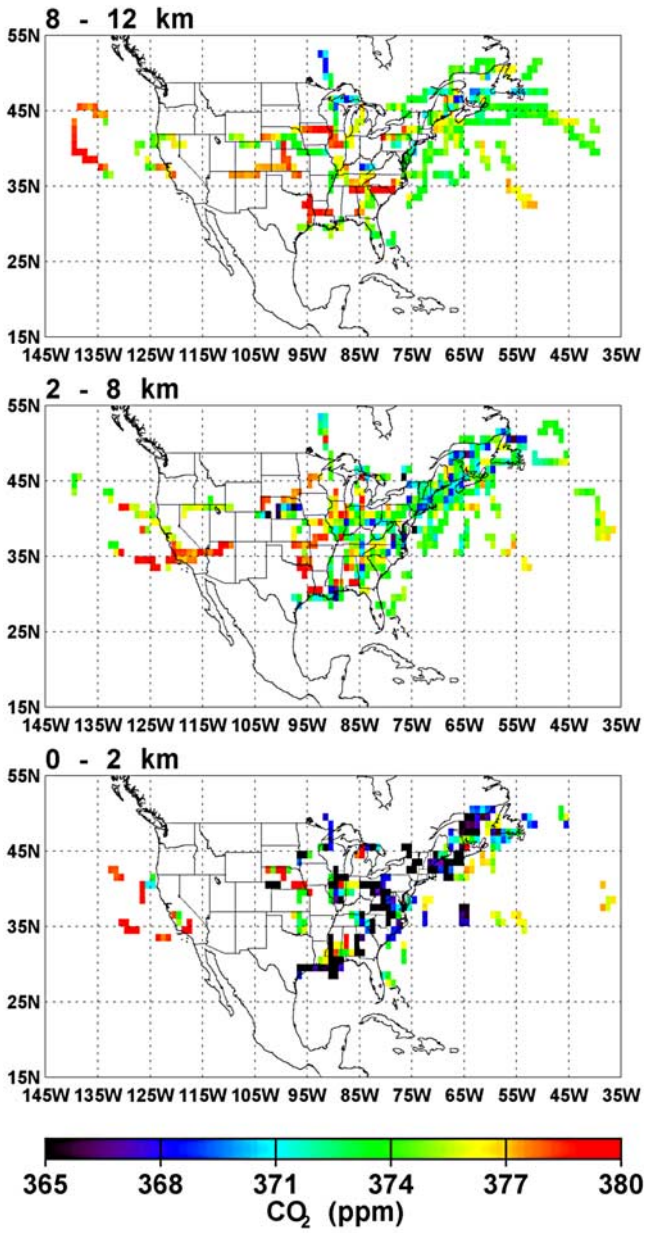

Figure 1. Regional distribution of CO_2 during INTEX-NA for the altitude regime of 0–2 km, 2–8 km, and 8–12 km. Data were grouped into 1° latitude by 1° longitude bins and then averaged.

7074.4 Tg of carbon dioxide equivalents, an increase of 15.8% from 1990 to 2004.

[3] Anthropogenic CO_2 emissions were partly offset by carbon sequestration in forests, trees in urban areas, and croplands at a rate of 11% of total emissions in 2004 [*EPA*, 2006]. Exchange with the terrestrial biosphere is mostly through uptake by photosynthesis and emission from plant respiration and decomposition of organic matter with seasonal variations. Many carbon cycle studies have indicated that the ocean and terrestrial ecosystems in the Northern Hemisphere are a net sink for atmospheric CO_2 at a rate of about 3 Pg C/year [*Bousquet et al.*, 2000; *Fung et al.*, 2005; *Goodale et al.*, 2001; *Myneni et al.*, 2001; *Nemani et al.*, 2003]. The budget for North America is the best constrained of any continent, with a mean uptake of 1.7 ± 0.5 Pg C/year [*Fan et al.*, 1998], mostly due to re-growth of logged forests and farmlands [*Turner et al.*, 1995], enhanced anthropogenic nitrogen deposition [*Holland et al.*, 1997; *Hudson et al.*, 1994; *Schindler and Bayley*, 1993; *Townsend et al.*, 1996], and the CO_2 fertilization effect [*Kheshgi et al.*, 1996].

[4] Beyond the fossil fuel contribution to anthropogenic emissions, wildfires also play an important role in the carbon cycle by affecting patterns of carbon accumulation and respiration in soils [*French et al.*, 2003; *O'Neill*, 2000; *O'Neill et al.*, 2002; *Richter et al.*, 2000], and represent a major global source of gases including carbon containing gases and aerosols emitted directly to the atmosphere particularly during high fire years [*Andreae and Merlet*, 2001; *Crutzen and Andreae*, 1990; *Liousse et al.*, 1996; *Logan et al.*, 1981; *Seiler and Crutzen*, 1980].

[5] During the summer of 2004, the Troposhperic Chemistry Program (TCP) at the National Aeronautics and Space Administration conducted the Intercontinental Chemical Transport Experiment–North America (INTEX-NA) airborne science mission [*Singh et al.*, 2006] to understand the impact of long-range transport of trace gases and aerosols on the changing chemical composition of the troposphere. Instrumentation for measurement of CO_2 was integrated on the NASA DC-8 research aircraft for INTEX-NA to examine its large-scale distribution and to provide insight into the factors influencing its summertime distribution over North America and adjacent oceans.

2. Study Region and Sampling Method

[6] During the July 1st through August 14th 2004 deployment, high temporal resolution (1 s) in situ CO_2 measurements were recorded aboard the DC-8 providing observations over sparsely sampled areas of North America and the North Atlantic. Eighteen science flights were conducted from three major hubs: Dryden Flight Research Center, CA; Mid-America Airfield, IL; and PEASE International Trade-Port, NH. Airborne surveys were flown over a large area bounded by 36°–139°W longitude and 27°–53°N latitude and included sampling between the 0.15–12 km altitude. Flights were conducted during the day and generally during fair weather.

[7] A modified LI-COR model 6252 non-dispersive infrared gas analyzer was used to determine CO_2 mixing ratios. This dual cell instrument achieves high precision by measuring the differential absorption between sample air and a calibrated reference gas that is traceable to the World Meteorological Organization primary calibration standards. The system was operated at constant pressure (250 torr) and had a precision of ±0.1 ppm (1 sigma) and accuracy of ±0.25 ppm. Experimental procedures are described in detail by *Anderson et al.* [1996] and *Vay et al.* [1999, 2003]. Complementary data used here from numerous instruments has a long history of inclusion in the NASA DC-8 TCP payload, and the techniques were essentially identical to those previously described by *Jacob et al.* [2003]. Our analysis utilized data for in situ CO, O_3, C_2H_2, C_2H_6,

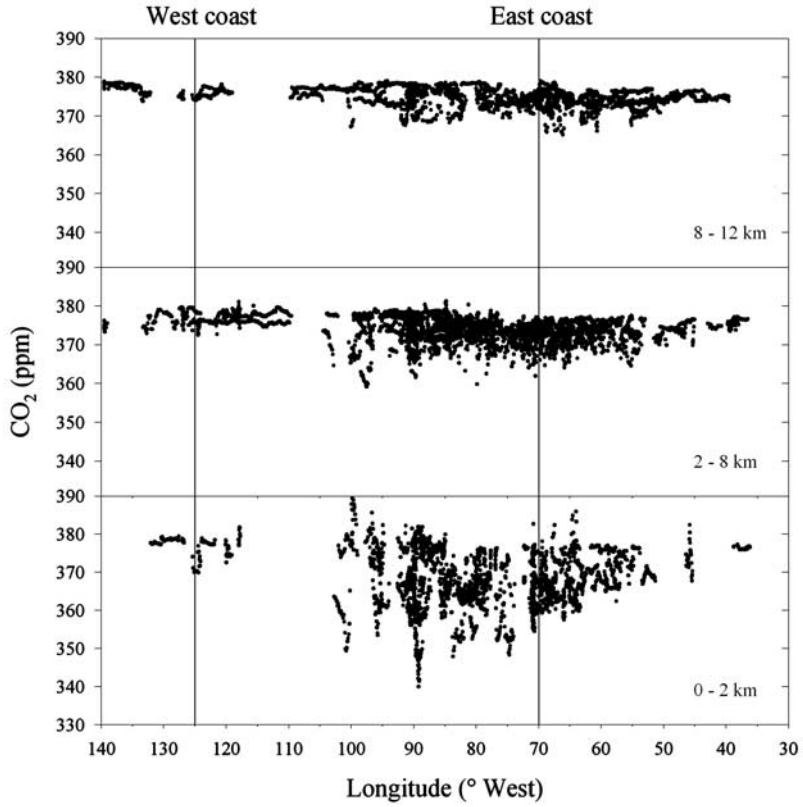

Figure 2. Dominance of the terrestrial biospheric uptake during summer can be seen in the longitudinal distributions of atmospheric CO_2 observed during INTEX-NA for the lower, mid, and upper troposphere.

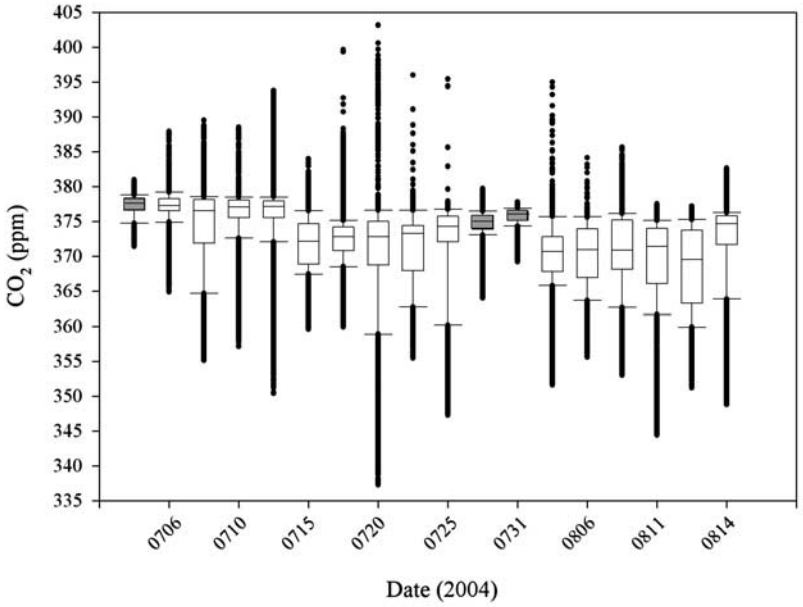

Figure 3. Distribution of CO_2 as a function of flight date. The CO_2 signal observed in flights over the ocean (shown in gray scale for the 1st, 28th, and 31st July flights) exhibited significantly less variability than those over land, demonstrating the influence of active CO_2 sources and sinks on the measurements.

Table 1. Summary of Carbon Dioxide Measurements Obtained on Board the DC-8 During the INTEX-NA Field Mission Conducted From 1 July to 14 August, 2004

Flight Date, yyyymmdd	Mean ± 1σ, ppm	Median, ppm	CO_2 Range, ppm	Latitude (°N) Range	Longitude (°W) Range
20040701	377.3 ± 1.5	377.7	371.4–380.1	33.5–45.0	139.5–117.8
20040706	377.2 ± 2.0	377.3	364.9–387.9	35.0–45.9	118.0–84.1
20040708	374.3 ± 5.5	376.6	354.2–388.8	34.2–42.5	103.9–77.7
20040710	376.1 ± 3.2	377.1	357.1–388.5	30.1–42.1	95.6–76.1
20040712	376.1 ± 4.6	377.2	350.4–393.8	31.3–46.3	100.0–82.9
20040715	371.9 ± 3.5	372.1	362.9–384.0	38.9–53.1	92.2–71.5
20040718	372.4 ± 3.1	372.9	360.0–387.8	43.3–52.9	70.6–45.1
20040720	370.1 ± 7.7	372.8	337.3–403.2	32.8–43.3	90.0–70.9
20040722	371.4 ± 4.8	373.3	357.7–383.5	35.3–51.7	72.7–59.8
20040725	372.3 ± 6.2	374.4	347.3–377.9	27.5–44.7	86.9–70.2
20040728	374.8 ± 1.2	374.8	371.4–377.5	37.6–45.6	71.1–36.2
20040731	375.8 ± 1.2	376.2	369.2–377.8	32.0–46.7	71.0–51.8
20040802	370.3 ± 4.3	370.7	351.6–379.8	41.8–51.5	77.0–50.1
20040806	370.3 ± 4.5	371.2	355.7–384.1	32.3–43.1	90.1–68.3
20040807	370.9 ± 4.8	370.9	353.6–385.7	41.6–51.0	72.4–55.7
20040811	369.7 ± 5.7	371.5	344.4–377.5	35.7–46.9	89.5–64.5
20040813	368.9 ± 5.8	370.4	354.3–377.2	28.8–38.4	97.0–88.3
20040814	372.6 ± 5.2	374.7	348.8–381.6	35.1–42.0	125.4–90.1

C_2Cl_4, CH_2O, NO_2, CH_3OH, CH_3CN, PAN, and HCN. Mission and meteorological descriptions are given by *Singh et al.* [2006] and *Fuelberg et al.* [2007], respectively.

3. Results and Discussion

3.1. Regional-Scale and Vertical Distributions of CO_2

[8] The spatially averaged CO_2 distribution (Figure 1) displays substantial variability reflecting not only the biospheric uptake in the northern summer, but also the preponderance of human population and industrial activity in the northern hemisphere. These data, plotted as averages within 1° latitude by 1° longitude bins, coarsely represent three different regimes within the troposphere: 0–2 km (Planetary Boundary Layer (PBL)), 2–8 km (mid-troposphere), and 8–12 km (upper troposphere (UT)). August and September are the time of maximum CO_2 uptake in the northern hemisphere in the high and midlatitude regions [*Conway et al.*, 1994]. These biospheric uptake features are shown distinctively in the PBL bin between the 30–50°N and east of 90°W over the continent. The lowest CO_2 mixing ratios (337 ppm minimum) were observed near the surface over the mid-continental agricultural-intensive states of Illinois and Nebraska. Higher CO_2 mixing ratios are evident in the free troposphere (FT) as well as an east-west gradient demarcated by the Mississippi River. The trend toward higher CO_2 values with altitude reflects remnants of an earlier seasonal cycle that is out of phase with the lower tropospheric signal by 1–3 months; the average time for transport processes to communicate the surface signal throughout the tropospheric column [*Nakazawa et al.*, 1991]. Moreover, convection, stratospheric intrusions, long-range transport (LRT), and wildfires were factors contributing to the variability observed in the FT and will be discussed in later sections.

[9] Dominance of the terrestrial biospheric uptake during summer can be seen in the longitudinal distribution of atmospheric CO_2 shown in Figure 2. With increasing distance from the east coast, the biospheric signal becomes less evident as it dilutes into the regional background over the Atlantic Ocean. Clear signatures of CO_2 uptake were also seen in the lowest 2–3 km with a diminished gradient with altitude over land. Higher average CO_2 mixing ratios recorded on flights west of the Mississippi River, likely reflect less active vegetation in the dry western part of the country. From the CO_2 distribution for individual flight days (Figure 3), differences in the CO_2 spatial variability over land versus ocean are apparent. The largest change in CO_2 mixing ratios was observed over the continent (66 ppm) on the July 20th flight. This is in contrast to flights over the Atlantic that exhibited substantially less variability, evident by the compactness of the July 31st data. Statistics for each flight are summarized in Table 1 and reveal median CO_2 mixing ratios that decrease with time (377 to 370 ppm) as sampling progressed deeper into the growing season. Minimum CO_2 values for individual flights often occurred $\leq$1 km and >35 °N.

[10] Perhaps the best view of the influence of the continent on the CO_2 concentration distributions can be seen in Figure 4 where the data are presented for flights upwind of North America, over, and downwind of the continent. On July 1st, measurements were made over the eastern North Pacific preceding deployment to INTEX-NA intensive sites providing a glimpse into upstream CO_2 concentration fields. Here CO_2 mixing ratio observations varied by 7 ppm versus 66 ppm over the continent, exhibiting ~2% variability compared to 18% over land. Within the boundary layer, median values were 378 ppm for the Pacific, 366 ppm for the land, and 369 ppm over the western North Atlantic capturing well the influence of terrestrial ecosystems on the observations. Conspicuous is the seeming absence of a notable anthropogenic perturbation over the continent however, the anthropogenic signal is embedded within the observations, obscured by the seasonal activity of the biosphere. A new CO tracer method has been introduced by *Campbell et al.* [2007] to disentangle the anthropogenic and biogenic signals within the INTEX-NA data set.

[11] Current knowledge about global CO_2 sources and sinks has been derived principally from the distribution of atmospheric CO_2 concentrations, often using inverse modeling approaches [*Gurney et al.*, 2002]. In principle, it is

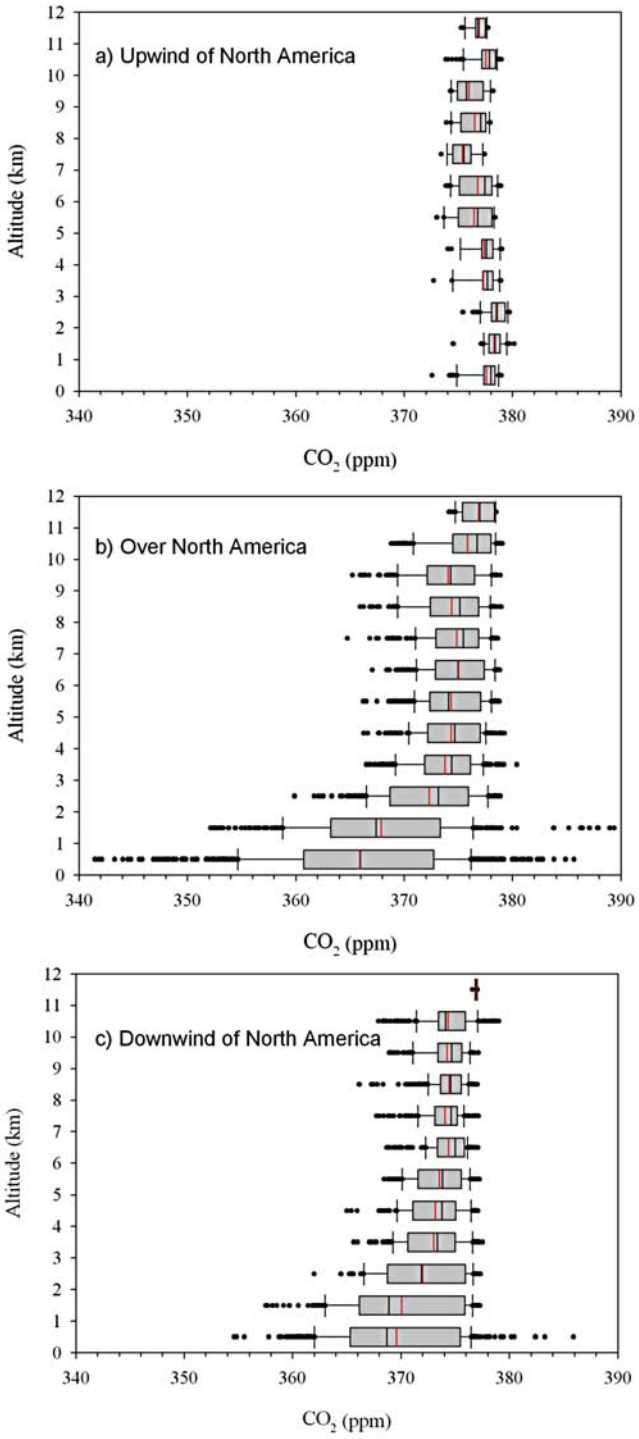

Figure 4. Distribution of CO_2 mixing ratios for measurements made over (a) the eastern North Pacific Ocean (b) North America and (c) the western North Atlantic showing the distinct influence of the continent on the observed variability. Vertical lines in each box represent the mean (red) and median (black) values.

possible to estimate CO_2 surface fluxes from atmospheric CO_2 concentration, provided that atmospheric transport can be accurately modeled. Presently, regional carbon budgets are reconstructed from measurements conducted at ~100 observing stations [*Chedin et al.*, 2003] spread inhomogeneously across the globe thus posing a constraint on the reliability of fluxes estimated at sub-continental scales [*Gurney et al.*, 2004; *Kaminski et al.*, 1999; *Rodenbeck et al.*, 2003]. Using only the surface CO_2 observations for this analysis yields an inferred carbon flux that is highly sensitive to the details of the boundary layer dynamics in the transport model [*Gurney et al.*, 2004]. One possible way to reduce the sensitivity of these inversions to poorly represented boundary layer dynamics is to use CO_2 vertical profiles and/or column measurements in addition to surface observations [*Stephens et al.*, 2007; *Yang et al.*, 2002]. Moreover, the effect of vertical transport on CO_2 concentrations near the surface is a major uncertainty in estimating net regional carbon fluxes therefore free tropospheric measurements are beneficial for evaluating model mixing and the resulting flux estimates [*Krakauer et al.*, 2005] (web ppt file).

[12] During INTEX-NA, vertical soundings executed by the DC-8 permitted characterization of CO_2 variations at relevant scales for resolution of atmospheric models and satellites. Vertical profile data acquired during two of the eighteen science flights (Figure 5a) illustrates differences

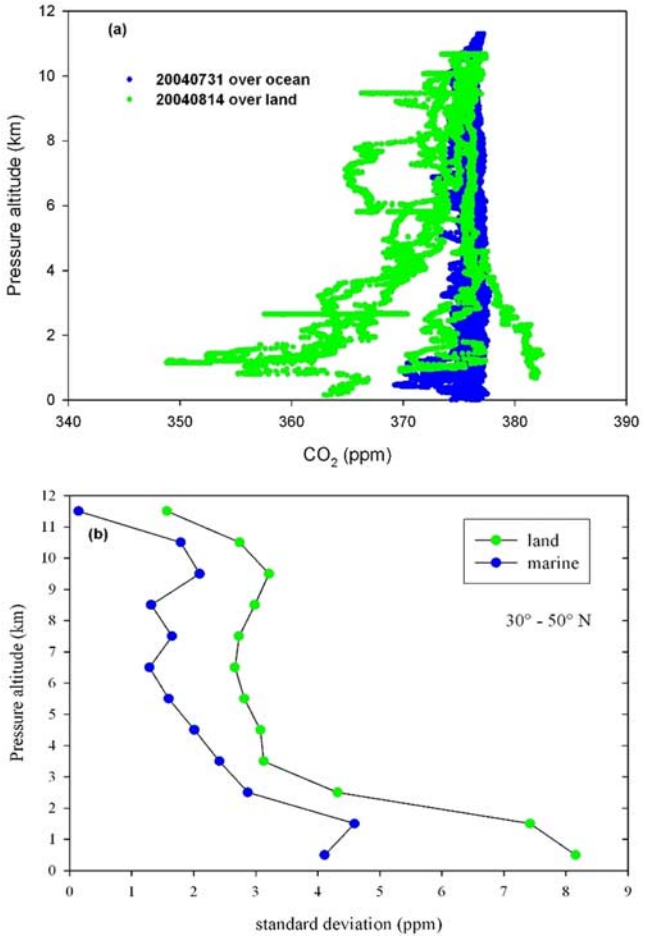

Figure 5. (a) CO_2 vertical distributions over the continent and the Atlantic Ocean without averaging effects. (b) Standard deviation of the mean land and marine profiles.

observed in the atmospheric column over the continental U.S. versus the North Atlantic Ocean. When comparing signatures over the ocean versus land, CO_2 varied <1% in the atmospheric column probed (e.g., July 31st, 2004 (20040731)) compared with 10% (e.g., 20040814), respectively. In the heavily under-sampled mid-to-upper troposphere, where the AIRS instrument on the Aqua satellite is mainly sensitive to CO_2, sampling of a highly heterogeneous tracer field is evident. Figure 5b characterizes well CO_2 variations in the vertical dimension for the entire mission data set and shows that the CO_2 signal in the column is dominated by the boundary layer and surface emissions/uptake. In the marine case, the variability of CO_2 below 2 km is, in part, influenced by continental outflow above the Marine Boundary Layer (MBL). In situ observations in the upper troposphere show a higher degree of variability (9–10 km bin) than in the mid-troposphere over both land and ocean. The altitude profile variability of bin-averaged CO_2 data reveals that a precision of ~1% is necessary for a space-based sensor with maximum sensitivity in the mid-troposphere to resolve the CO_2 signal. The ocean-land separation potentially lends insight into differences observed in retrievals over the land compared to the oceans in the extra-tropics and may be beneficial for future retrieval algorithm development/refinement and calibration/validation of evolving remote CO_2 sensors [*Washenfelder et al.*, 2006].

3.2. Influences on Spatial Variability

[13] Measurements of atmospheric composition provide powerful constraints to improve understanding of surface fluxes of trace compounds and their subsequent fate in the atmosphere [*Palmer et al.*, 2006]. Given that concentrations of atmospheric constituents observed by aircraft have inevitably been influenced by the interaction between atmospheric transport and the spatial and temporal variation of sources and sinks, we invoke CO_2 along with other simultaneous trace gas measurements and supporting meteorological data in the ensuing sections to elucidate the various anthropogenic, natural, and dynamical influences on the observed variability of CO_2 during INTEX-NA.

3.2.1. Biospheric Influence

[14] Since terrestrial ecosystems are major sources and sinks of carbon, quantifying their role in the continental carbon budget requires an understanding of both fast (hours to days) and longer-term fluxes (years to decades). To quantify and understand the variations in CO_2 behavior between the planetary boundary layer and the free troposphere, and to link the aircraft measured CO_2 variations in the troposphere to terrestrial landscape sources of carbon flows and fluxes for major land cover type, CO_2 measurements were explored with remote-sensing data products and GIS-based methods. Several derived products from the LANDSAT, NOAA AVHRR, and MODIS sensors were used to specify spatiotemporal patterns of land use cover and vegetation characteristics. In particular, MODIS products available from daily (e.g., surface reflectance) to 8-day (e.g., Gross Primary Productivity (GPP)) to monthly (e.g., Leaf Area Index (LAI)) to annual (e.g., Net Primary Productivity (NPP)) temporal resolutions were effectively utilized for characterizing the carbon flows and fluxes over heterogeneous landscapes.

[15] Ideally, aircraft measurements of CO_2 can be separated into portions of flux records representing the land cover types through just averaging the CO_2 values for all cover types involved. However, such separation maybe misrepresentative, as (a) different land cover types are often spatially mixed and heterogeneous in a given area, (b) wind further mixes the CO_2 fluxes to and from adjacent land cover types (e.g., forest versus crop), and (c) land cover areas of the same cover type at different distances from the aircraft in the wind direction may contribute differently to the flux. To elucidate the variability in the observed CO_2 mixing ratios, data were averaged based on the distance-weighted cover fraction approach [*Chen et al.*, 1999]. Using latitude and longitude information coincident with the CO_2 measurements from the aircraft data, we first geo-referenced the land use cover data derived from LANDSAT. We then spatially averaged the CO_2 mixing ratio data along the flight track based on the distance-weighted land cover type fraction for each flight segment according to the aircraft speed and direction. For example, for the July 20th boundary layer run over Illinois (Figure 6a), at a nominal aircraft groundspeed of 180 $msec^{-1}$, a sampling distance of about 151 km was covered and corresponded to nearly 5036 pixels in the LANDSAT data. The airborne CO_2 data was partitioned and averaged based on individual flight segments over different land cover types to infer variations. Although there are important mass balance approaches such as the atmospheric boundary layer budget method for accounting for CO_2 variations, we could not attempt the same due to measurement limitations (e.g., vertical velocity of the Atmospheric Boundary Layer (ABL) growth (w_+); surface aerodynamic roughness; atmospheric stability parameters; etc. were unavailable). Nonetheless, we were able to observe some significant trends such as low CO_2 mixing ratios in agricultural regions through the distance-weighted averaging approach.

[16] The result from the above analysis shows that variations in CO_2 mixing ratios at lower altitudes were attributed to terrestrial sources of vegetation cover that is highly heterogeneously occupying the landscape (Figure 6b). Interclass variations in CO_2 mixing ratios between different vegetation types suggested averaged lower CO_2 mixing ratios for corn crop compared to others (the averaged CO_2 concentrations were 338–345 ppm for corn, 348–354 ppm for soybeans, and 352–360 ppm for pasture and woodlots). This is mainly attributed to the C4-dicarboxylic acid pathway of carbon fixation in corn, having a higher rate of photosynthesis than other C3 plants such as soybeans [*Crosbie et al.*, 1977; *Curtis et al.*, 1969; *Ehleringer and Pearcy*, 1983; *Prueger et al.*, 2004].

[17] In addition to LANDSAT derived biophysical products, MODIS Normalized Difference Vegetation Index (NDVI) products were utilized in this study. NDVI is an indicator of vegetation activity where values near 0 indicate very sparse vegetation and dense vegetation is indicated by values approaching 1. For the July 20th case study over Illinois, low CO_2 mixing ratios were found to correlate well ($R^2 = 0.87$) with vegetation density (Figure 6c). Although these results suggest significant biospheric uptake of CO_2 from vegetation, a more thorough analysis is required. For example, *Wang et al.* [2007] has recently shown that atmospheric CO_2 variations are dominated by coherent

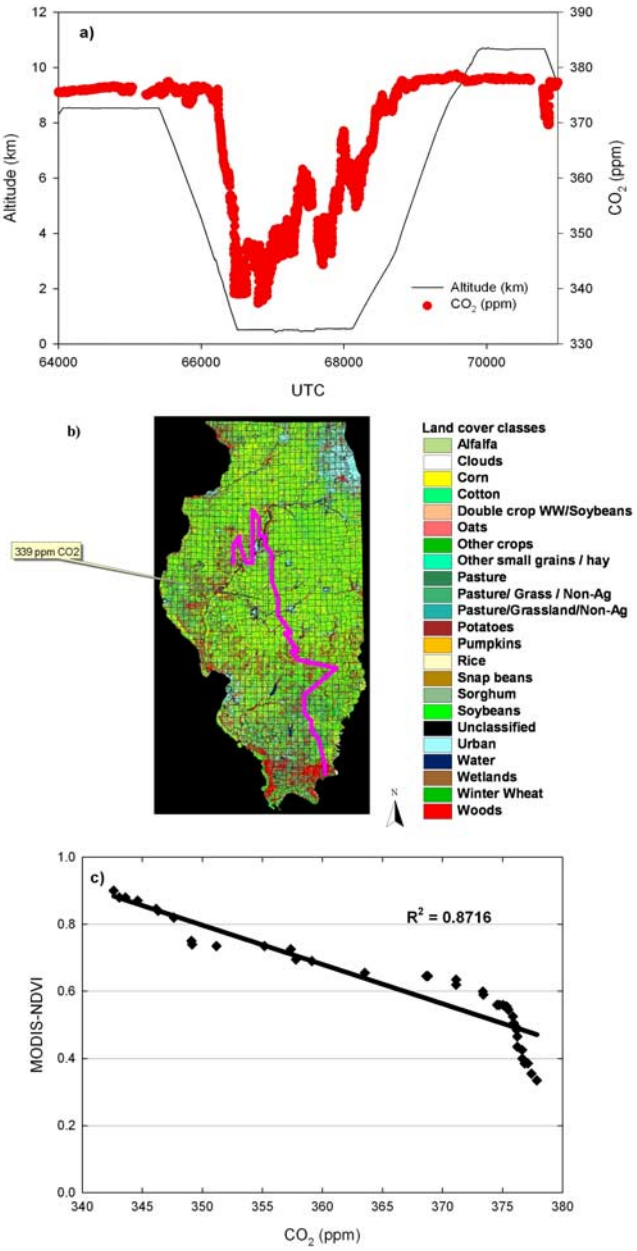

Figure 6. (a) The lowest CO_2 mixing ratios observed during INTEX-NA were over agricultural fields in Illinois on 20th July (b) Flight path overlay on LANDSAT map and airborne CO_2 data for Level II classes of land cover. (c) Relationship between MODIS derived NDVI and aircraft based in situ CO_2 measurement data.

regional anomalies of up to several 10s of ppm by surface weather (especially temperature, humidity, and radiation) and advection by synoptic-scale winds. For addressing these issues, models involving atmospheric transport are required to be able to generate fine-resolution transport information to resolve the high frequency airborne CO_2 data sets and to quantify regional scale CO_2 sources and sinks [*Wang et al.*, 2007].

3.2.2. Convective Influence

[18] The upper troposphere (UT) is only indirectly related to surface fluxes via lower troposphere transport, and thus the effect of surface fluxes on concentrations in this region is not entirely obvious [*Tiwari et al.*, 2006]. UT CO_2 is typically dominated by the interplay between fossil fuel emissions, and the seasonal cycle of carbon release and uptake by the land vegetation in the NH. It exhibits a similar seasonality as is observed near the ground, but of a lower magnitude with $\sim$1 month time delay compared to the surface fluxes. Convective storms, however, represent an important mechanism for the vertical redistribution of atmospheric CO_2 on much shorter timescales; less than one hour compared to weeks or months [*Dickerson et al.*, 1987]. Deep convection such as occurs in summertime thunderstorms is a highly efficient mechanism for the fast transport of air near the Earth's surface to the UT [*Chatfield and Crutzen*, 1984; *Dickerson et al.*, 1987; *Hauf et al.*, 1995; *Pickering et al.*, 1988]. Typical convective storms have spatial scales of tens of kilometers and vertical velocities as large as 15 m sec^{-1} [*Dye et al.*, 2000], making their local influence in the UT extremely strong. Although convection may account for only a small percentage of the mass of lower tropospheric air mixed into the UT, the chemical impact can be significant because Boundary Layer (BL) air has a much different chemical composition than the free troposphere [*Mullendore et al.*, 2005].

[19] Convection occurring during the summer of 2004 was examined to determine its influence on the distribution of CO_2 over the INTEX-NA sampling domain. Several studies show that the Upper Troposphere/Lower Stratosphere (UT/LS) was greatly influenced by convective processes during the mission: 13% by *Liang et al.* [2007], 12% by (J. A. Al-Saadi et al., A lagrangian characterization of the sources and chemical transformation of air influencing the US and Europe during the 2004 ICARTT/INTEX-A Campaign, submitted to *Journal of Geophysical Research*, 2006, hereinafter referred to as J. A. Al-Saadi et al., submitted manuscript, 2006), and 12.5 % by *Fuelberg et al.* [2007] and that convective outflow was strongest between 9.5 and 10.5 km [*Bertram et al.*, 2007]. Here, we document the occurrence of a series of convective episodes during INTEX-NA and present trace gas measurements from the penetrations of convective clouds. Since the CO_2 concentration is lower in the BL during the Northern Hemisphere (NH) summer compared to aloft, we use this difference in CO_2 mixing ratio to identify air masses convectively transported from the BL to the UT [*Huntrieser et al.*, 2002]. Figure 7 captures vertical profiles of several trace gases (CO_2, CO, NO_2, CH_2O, C_2H_6, and C_2Cl_4) simultaneously measured in convectively influenced air parcels sampled during the July 12th flight over the continental U.S. These vertical profiles were considered together with convective influence forecast plots (http://bocachica.arc.nasa.gov/INTEX/coninf_plots.html) and corresponding DC-8 flight track (Figure 8). The coupling of the convective influence calculations with the tracer data indicates that the BL tracers were carried upward in the core of the updraft to the UT within hours of sampling by the DC-8, experiencing little dilution (Figure 7a); in less than a day (Figure 7b); and in 1 to 2 days (Figure 7c). In the fresh convection case (Figure 7a), CO_2 concentrations <375 ppm were observed in the BL and throughout the UT (e.g., 8, 9.5 and 12 km). Concomitant increases in CO, C_2Cl_4, C_2H_6 in the UT having concentrations similar to those measured in BL air, substan-

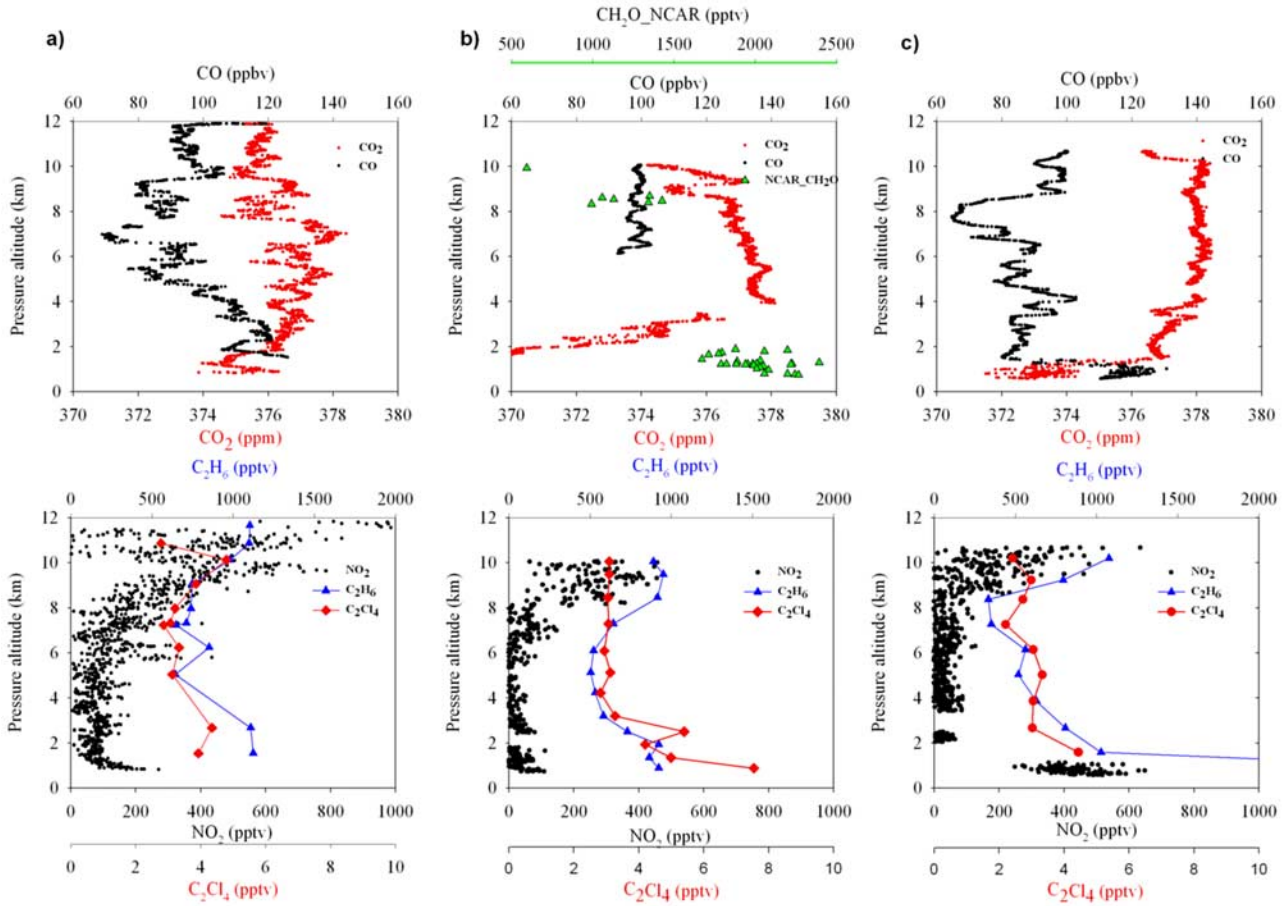

Figure 7. Vertical profiles of several trace gases (CO_2, CO, NO_2, CH_2O, C_2H_6, and C_2Cl_4) simultaneously measured in convectively influenced air parcels (a) within hours (b) in less than a day (c) in 1 to 2 days during on 12th July.

tiates vertical transport of chemical species in a convective environment. Similarly for the <1 day old case (Figure 7b) where CO_2 depleted air sampled at 9 km corresponds with enhanced CH_2O and C_2H_6. Observations over Oklahoma while penetrating a convective cell > 1 day old (Figure 7c) suggest that sufficient time has elapsed for dilution of CO_2 to occur in the UT compared with C_2H_6 that still conveys evidence of convective transport. From observations of CO_2

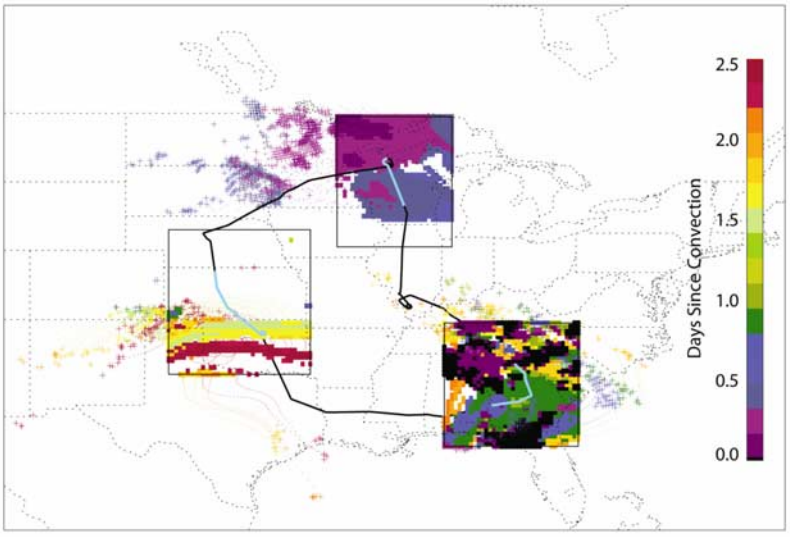

Figure 8. Convective influence forecast (NASA Ames) plots with DC-8 flight track.

Figure 9. Alaskan ecoregions and fire. The 2004 fire scars, shown in red, are taken from the Bureau of Land Management (http://agdc.usgs.gov/data/blm/fire/index.html). HMS-based MODIS data, shown in black, are from the 9 days that preceded the 18th July flight.

during INTEX-NA, *Bertram et al.* [2007] calculated that the fraction of BL air in fresh convection was 0.11 ± 0.03.

[20] When pollutants are released in or transported to the UT, the longer lifetimes and higher wind speeds greatly expand their range of influence [*Dickerson et al.*, 1987]. Since CO_2 has an atmospheric lifetime on the order of hours to years, rapid convective transport may inevitably play a crucial role in defining the UT global distributions.

3.2.3. Biomass Burning Influences

[21] Exceptionally hot and dry conditions in the boreal region of Alaska and western Canada were a prelude to the severe summer 2004 wildfire season that affected U.S. air quality via the long-range transport of fire emissions (A. Clarke et al., Biomass burning and pollution aerosol over North America: Organic components and their influence on spectral optical properties and humidification response, submitted to *Journal of Geophysical Research*, 2006; P. Cook et al., Forest fire plumes over the North Atlantic: p-TOMCAT model simulations with aircraft and satellite measurements from the ITOP/ICARTT Campaign, submitted to *Journal of Geophysical Research*, 2006; W. W. McMillan et al., AIRS views of transport from 12–22 July 2004 Alaskan/Canadian fires: Correlation of AIRS CO and MODIS AOD with forward trajectories and comparison of AIRS CO retrievals with DC-8 in situ measurements during INTEX-A/ICARTT, submitted to *Journal of Geophysical Research*, 2006; A. L. Soja et al., Description of a ground-based methodology for estimating boreal fire emissions for use in regional and global scale transport models, submitted to *Journal of Geophysical Research*, 2006, hereinafter referred to as A. L. Soja et al., submitted manuscript, 2006). Most of fires burned in the Intermontane Boreal forest (Figure 9) which holds the second largest carbon stock in North American boreal eco-zones [*Bourgeau-Chavez et al.*, 2000; A. L. Soja et al., submitted manuscript, 2006]. Fifteen to twenty percent of the total global carbon emissions from biomass burning [*Amiro et al.*, 2001; *Cahoon et al.*, 1994; *Conard et al.*, 2002; *French et al.*, 2000; *Kasischke and Bruhwiler*, 2002; *Soja et al.*, 2004] are emitted from these zones as the peatlands and soil organic matter (SOM) they contain represent a vast terrestrial carbon reservoir [*Alexeyev and Birdsey*, 1998; *Apps et al.*, 1993; *Zoltai and Martikainen*, 1996] available for release to the atmosphere during fire [*Kasischke and Johnstone*, 2005; *Soja et al.*, 2004; *Turetsky et al.*, 2004]. Indeed, *Turquety et al.* [2007] and *Pfister et al.* [2005] reported that 30 Tg CO including 11 Tg CO from peat were emitted from the 2004 fires.

[22] Surface burning products injected into the UT and/or LS [*Damoah et al.*, 2006; *Turquety et al.*, 2007] by pyro-convection were transported eastward and southeastward with the jet stream [*Fuelberg et al.*, 2007] and subsequently sampled by the DC-8. Figure 10 depicts enhanced CO_2 (2.7 ppm) and CO (442 ppbv) in an air mass sampled at 7 km over the western North Atlantic on July 18th. The plume was also augmented with elevated CH_3CN, PAN, HCN, and H_2CO which is indicative of combustion contributions from biomass burning. A Modified Combustion Efficiency (MCE = $\Delta CO_2/(\Delta CO_2 + \Delta CO)$ value of 0.86 was calculated for this plume indicating a smoldering combustion source [*Korontzi et al.*, 2003; *Sinha et al.*, 2003; *Ward et al.*, 1996; *Yokelson et al.*, 1999]. Four other discrete plumes investigated showed a mix of smoldering (0.75–0.85 MCE) and flaming (0.97–0.99 MCE) combustion with MCE values ranging from 0.93 to 0.98. Kinematic backward trajectories calculated along the INTEX-NA flight tracks by the Florida State University group show however, these air parcels contacted the surface prior to sampling. Thus these higher MCE values likely reflect

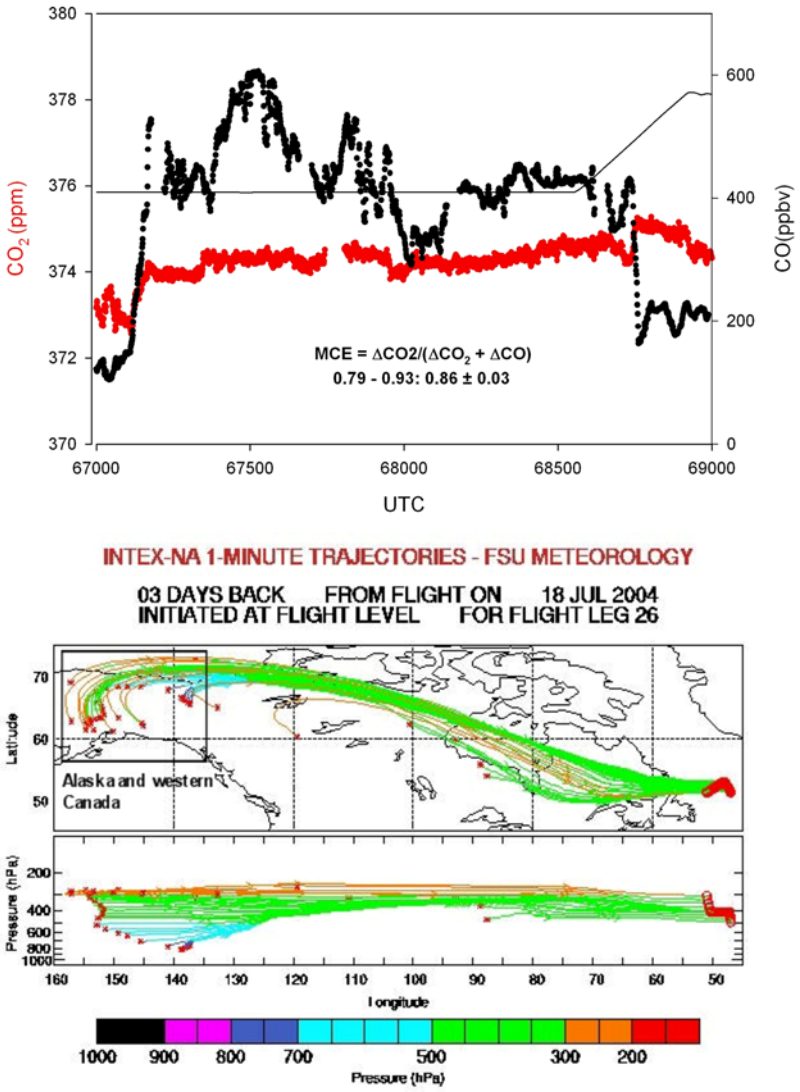

Figure 10. Fire emissions originating from Alaska as observed over the Northwestern Atlantic at 7 km on 18th July (top panel) and their transport history (bottom panel).

fire emissions that have undergone mixing/dilution with transport.

[23] These results support the recent shift from using the traditional flaming to smoldering ratio of 50:50 to 20:80 or 10:90 for calculating trace gas emissions from boreal SOM and peatland burning [*French et al.*, 2003; *Kasischke and Bruhwiler*, 2002; *Soja et al.*, 2004]. An increase in the smoldering proportion of this ratio represents an increase in trace gas emissions of CO, CH_4 and NMHC, accounting for the unique fuels stored for decades to centuries in boreal ecosystems. Since biomass burning in this region is predicted to increase under current climate change scenarios and has been corroborated in recent reports [A. L. Soja et al., submitted manuscript, 2006; *Stocks et al.*, 1998], knowledge of the percentage of trace gases emitted to the atmosphere could become increasingly important. These results could play an essential role in the carbon inventory and in simulation transport models, because carbon released from biomass burning is significant, particularly during severe fire seasons like those in 2004.

3.2.4. Stratospheric Influence

[24] Variations in stratospheric CO_2 are mainly a reflection of tropospheric transport on surface concentrations. They contain the signature of the seasonal variation of the lower tropospheric environment and the annual increase although the signal is generally weaker $\sim$2–3 ppm) and somewhat lagged (1–2 months) compared to the surface signal [*Boering et al.*, 1994; *Hall and Prather*, 1993; *Nakazawa et al.*, 1991]. Through various atmospheric transport pathways and dynamical processes such as stratospheric intrusions and cut-off lows, subsequent exchange with the free troposphere can occur.

[25] With the INTEX-NA period dominated by low-pressure conditions over northeastern North America, the free troposphere in that region was frequently enriched by stratospheric O_3 [*Thompson et al.*, 2007]. Estimates from several studies of the stratospheric contribution to the upper

Table 2. Statistics for CO_2 and Other Tracers When O_3 Mixing Ratios Exceeded 200 and 300 ppbv Within the Upper Troposphere

	Latitude (°N)	Longitude (°W)	Altitude, km	CO_2, ppm	CO, ppbv	O_3, ppbv	H_2O, ppmv
>200 ppbv O_3							
Mean ± 1σ	43.0 ± 4.5	70.8 ± 7.9	9.6 ± 0.8	375.1 ± 0.8	58.7 ± 13.7	286.4 ± 61.7	49.7 ± 29.9
Median	42.4	71.5	9.5	375.4	69.4	267.2	47.5
Minimum	35.3	90.2	8.2	371.9	35.0	200.1	8.6
Maximum	50.1	60.5	11.3	377.1	91.6	447.0	261.4
>300 ppbv O_3							
Mean ± 1σ	46.9 ± 3.5	66.2 ± 6.1	10.1 ± 0.4	375.9 ± 0.2	44.3 ± 5.4	356.1 ± 37.5	19.6 ± 7.7
Median	49.6	61.4	10.1	375.9	46.7	345.5	20.3
Minimum	42.0	75.0	9.4	375.1	35.0	300.2	8.6
Maximum	50.1	60.6	10.7	377.0	54.9	445.9	38.1

tropospheric signal ranged from 16–34 % [J. A. Al-Saadi et al., submitted manuscript, 2006; J. E. Dibb et al., Stratospheric influence on the composition of the MId- and upper troposhere over North America sampled by the NASA DC-8 during INTEX-A, submitted to *Journal of Geophysical Research*, 2006, hereinafter referred to as J. E. Dibb et al., submitted manuscript, 2006; *Fuelberg et al.*, 2007; *Thompson et al.*, 2007]. Examination of the standard deviation of the mean CO_2 profiles illustrated in Figure 5b reveals greater variability in the high altitude data compared to the mid-levels for both ocean and land cases, likely a consequence of this contributing influence.

[26] To investigate the CO_2 variations in stratospherically influenced air masses sampled, we filtered the INTEX-NA data set on O_3 > 200 ppbv and O_3 > 300 ppbv, the latter representing occasional, penetration of the lower stratosphere by the aircraft. This filter is substantiated by correspondingly decreased CO, H_2O mixing ratios and work by J. E. Dibb et al., submitted manuscript, 2006 using Beryllium-7 and the HNO_3/O_3 ratio to extract stratospherically impacted air masses from the INTEX-NA data set. Median CO_2 concentrations vary less than 1 ppm from the observed remote marine "background" value of 376.2 ppm, differing by 0.5 ppm between the two categories compared to a commensurate change in CO of 22 ppbv and 30 ppmv in H_2O (Table 2). The altitude range for these events was 8.2–11.3 km. Data for the Aug. 6th flight segment (Figure 11), acquired when the DC-8 traversed a deep trough that produced a low tropopause over North Carolina, shows characteristic signatures of the tracer relationships observed in stratospherically influenced air masses during the summer of 2004. As the O_3 mixing ratio increased, signifying an increasing stratospheric influence, CO_2 values were positively correlated with O_3, but anti-correlated with CO. During the NH summer, this relationship is to be expected given the phase delay and different amplitude of the CO_2 seasonality between the ground and UT/LS whereas, the fluxes of CO from the surface do not reverse sign seasonally or diurnally like CO_2.

[27] Measurements and studies have demonstrated that the stratospheric air influencing the INTEX-NA sampling domain above 7 km originated primarily over the central Pacific at high altitude (J. A. Al-Saadi et al., submitted manuscript, 2006) thus contributing to the observed CO_2 spatial variability in the UT. Transport in this region is important for understanding the distribution of greenhouse gases, predicting climate change, and understanding the chemical and radiative balance of this part of the atmosphere [*Ray et al.*, 1999].

3.2.5. Long Range Transport-Asian Pollution Influence

[28] During INTEX-NA, five distinct Asian pollution plumes were sampled by the DC-8 even though summertime trans-Pacific transport is generally inefficient due to slow large-scale flow compared to springtime, a period of

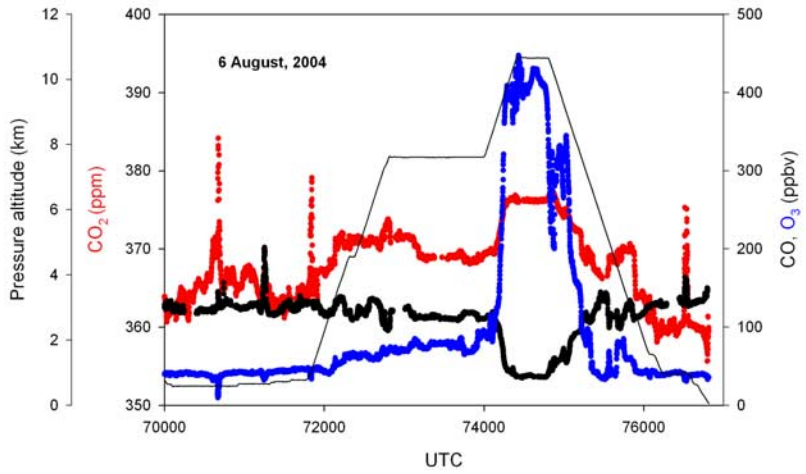

Figure 11. Time series for CO_2, CO and O_3 showing the stratospheric influence on measurements recorded in the upper troposphere.

Table 3. Observed CO_2 Composition and Transport Statistics of Five Asian Plumes[a]

Asian Plumes	Latitude (°N)	Longitude (°W)	Altitude, km	CO_2, ppm	Mean CO_2
1 Jul 2004					375.2
Leg1	36.2–37.0	132.1–133.4	8.2–10.7	373.6–376.8	375.4
Leg2	43.0–45.0	135.9–139-5	6.1–9.5	372.9–378.2	376.2
Leg3	43.2–43.9	133.0–133.7	6.4–9.2	373.4–377.3	374.9
Leg4	40.1–41.0	127.3–128.1	6.8–11.0	374.6–376.9	375.4
Leg5	40.5–40.7	126.8–127.1	6.8–10.7	373.4–376.2	374.7
Leg6	37.7–38.1	124.6–125.8	7.4–11.1	373.5–376.6	374.8
15 Jul 2004					372.8
Leg1	52.7–52.9	92.0–92.0	8.3–9.2	370.0–374.5	372.8
20 Jul 2004					372.0
Leg1	38.1–42.4	71.9–76.9	5.8–9.5	368.3–375.7	371.6
Leg2	39.5–41.4	76.5–80.5	6.4–8.3	369.3–375.0	372.3
2 Aug 2004					372.1
Leg1	47.4–47.8	68.0–70.6	9.7–10.1	371.4–373.9	372.0
Leg2	47.2–47.3	50.3–54.1	7.6–10.1	371.0–375.4	372.0
Leg3	44.1–46.2	60.3–62.6	6.4–9.2	368.5–374.2	372.4
Leg4	42.1–42.6	66.0–67.0	6.1–9.7	368.5–374.6	371.7
Leg5	43.7–43.9	69.4–69.8	6.4–9.0	371.1–374.7	372.6
14 Aug 2004					372.9
Leg1	39.1–39.7	92.3–95.6	8.7–10.1	371.8–375.0	373.3
Leg2	41.0–41.0	99.3–100.1	9.5–9.5	366.3–374.5	370.0
Leg3	41.0–41.0	122.9–123.8	10.7–10.7	374.9–375.8	375.3

[a]Asian plumes follow the time range identified by the observation-based Principal Component Analysis of *Liang et al.* [2007].

active cyclogenesis and strong westerly winds [*Andreae et al.*, 1988; *Berntsen et al.*, 1999; *Jacob et al.*, 1999; *Jaffe et al.*, 2003; *Kritz et al.*, 1990; *Nowak et al.*, 2004; *Parrish et al.*, 1992, 2004; *Yienger et al.*, 2000]. Time periods impacted by Asian emissions were identified by applying Principal Component Analysis (PCA) to the observations between 6–12 km [*Liang et al.*, 2007], and further substantiated by independent analyses with the GEOS-Chem model, and backward trajectories. Results for the five events are summarized in Table 3.

[29] The two strongest cases of sampling Asian continental outflow were on the July 1st and August 2nd flights conducted upwind and downwind of the continental U. S., respectively. The intercepted plumes were enhanced in trace gases associated with fossil fuel combustion (CO, C_2H_2), industrial (C_2Cl_4) and biospheric (CH_3OH) activity that can be invoked to elucidate the CO_2 signal in these events. Figure 12a shows vertical profiles of these chemical tracers on the July 1st flight when pollution originating in NE China was sampled over the Eastern Pacific. The CO_2 concentrations in this plume are often lower than the median CO_2 profile for this flight (Figure 12a) suggesting uptake by surface vegetation in Asia prior to convective lifting and transport. The plume also contains high levels of methanol which has a sizable biogenic source [*MacDonald and Fall*, 1993; *Schade and Goldstein*, 2006; *Singh et al.*, 2000].

[30] Deep convection over NE China and lifting in a typhoon east of Japan initiated LRT transport of Asian emissions prior to interception over the Gulf of Maine on August 2nd. The plume contains some mid-tropospheric (6–8 km) CO_2 concentrations that are below median values and correspond with CH_3OH enhancements (Figure 12b). Most however, are more representative of the observed free tropospheric CO_2 background values. The longer transport time (5–9 days) increases the likelihood of dispersion/dilution with travel over NA and/or mixing with stratospheric air along isentropic surfaces supported by higher $\Delta O_3/\Delta CO$ ratios [*Liang et al.*, 2007]. Comparatively fewer enhancements in C_2Cl_4 (τ = 68 days) along with the lesser biogenic signal supports contributions from different source regions than the July 1st case.

[31] Low CO_2 mixing ratios were recorded in all five plumes (Table 3) originating over continental East Asia. Observations of CO_2 depleted air containing elevated CO, C_2H_2, C_2Cl_4, and CH_3OH are consistent with mixing of biogenic emissions in the anthropogenic outflow. Estimates range from 7–11% for the influence from East Asia on the U. S. free troposphere composition during INTEX-NA [J. A. Al-Saadi et al., submitted manuscript, 2006; *Fuelberg et al.*, 2007; *Liang et al.*, 2007]. During the summer of 2004, we find that the East Asian influence is a contributor to the observed variability of CO_2 in the free troposphere and this seasonal export has possible implications for the North American carbon budget.

3.2.6. Continental Outflow to the North Atlantic Region

[32] Eastern North America, like other highly industrialized regions of the world, is a major source of atmospheric pollutants on a global basis [*Cooper et al.*, 2001; *Li et al.*, 2005; *Milne et al.*, 2000; *Whelpdale et al.*, 1984]. Although a large fraction of the pollutant mass emitted in such a region returns to the surface by the processes of wet and dry deposition, a significant amount is carried out of the region by the prevailing winds. These North American emissions are transported primarily into and removed from the atmosphere over the North Atlantic Ocean [*Stohl and Trickl*, 1999; *Whelpdale et al.*, 1984] by midlatitude cyclones propagating eastward and poleward before weakening south of Greenland [*Cooper et al.*, 2001; *Dickerson et al.*, 1995; *Merrill and Moody*, 1996; *Moody et al.*, 1996], heavily influencing the northeastern United States, Canadian Maritime Provinces, and Newfoundland [*Fehsenfeld et al.*, 1996; *Millet et al.*, 2006].

[33] North American outflow events were extracted from the INTEX-NA data set by examining air mass chemical signatures and backward trajectories. We identified seven

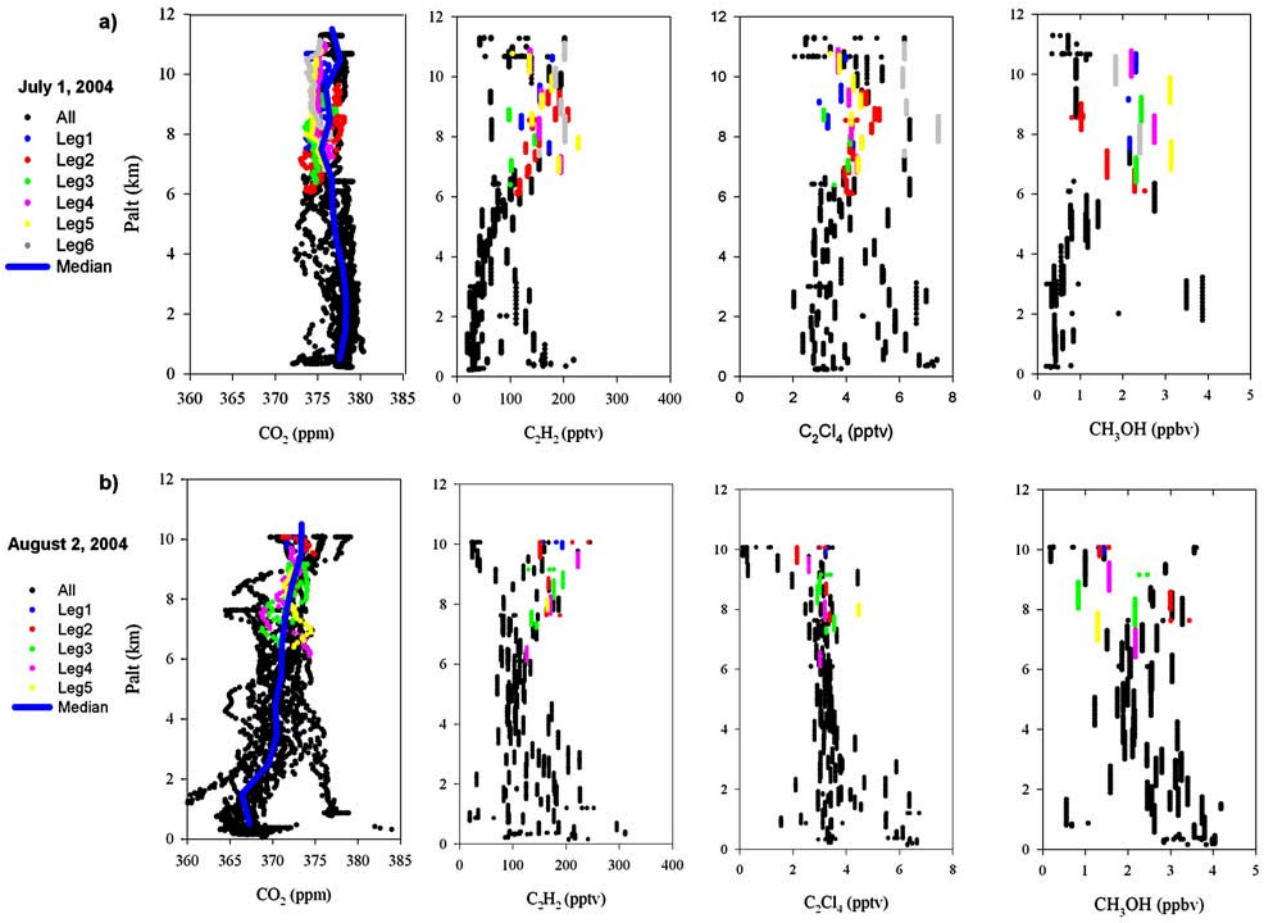

Figure 12. Vertical profiles of trace gases associated with fossil fuel combustion (C_2H_2), industrial processes (C_2Cl_4), and biogenic emissions (CH_3OH) sampled over the eastern Pacific during an Asian outflow event on (a) 1st July (Top) and (b) 2nd August (Bottom). Median observed vertical profile of CO_2 (blue line) and different time segments for Asian pollution events are highlighted in color.

distinct cases where air masses enriched in CO, O_3, SO_2, C_2Cl_4, and C_2H_2 yet depleted in CO_2 had originated over NA prior to sampling over the North Atlantic. An example is provided in a selected time series from the August 11th flight showing coincident enhancements in CO (140–180 ppb) and O_3 (60–97 ppb), while CO_2 $\leq$366 ppm (Figure 13). Kinematic 5-day backward trajectories reveals a transport pathway from the Great Lakes to the northeast at

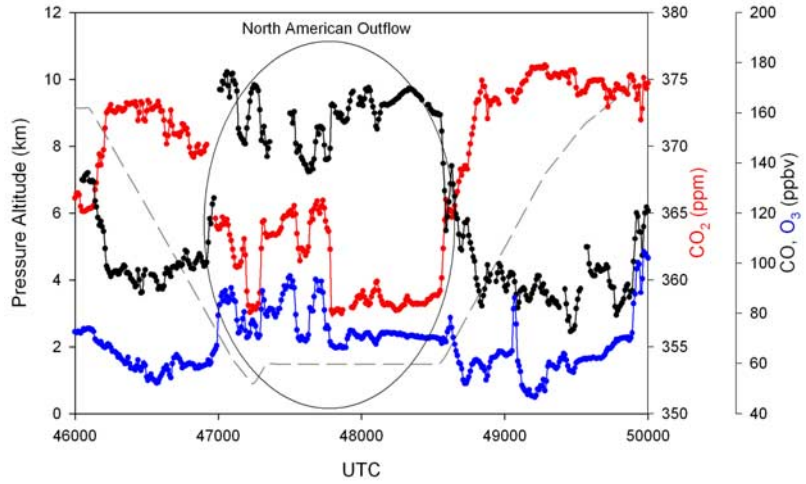

Figure 13. Time series for CO_2, CO, and O_3 during a U.S. outflow event (indicated by oval) sampled over the Bay of Fundy on 11th August.

$\geq$900 hPa with near-surface contact over much of the distance prior to sampling over the Bay of Fundy.

[34] Six of the seven outflow events were sampled north of 43°N and east of 70°W below 2.2 km, mostly within the BL. BL heights were established by examining coincident potential temperature and high resolution water vapor measurements. CO_2 mixing ratios in all of the outflow cases were 1% to 5% lower than the measured remote marine background value of 376.2 ppm. All of the events were associated with frontal activity which was more frequent than normal during INTEX-NA [*Fuelberg et al.*, 2007].

[35] In summary, both biogenic and anthropogenic signals were captured in North American outflow transported downwind of the continent contributing greatly to the variability of atmospheric CO_2 observed within the BL beyond 43°N. In opposite seasons, when winter air mass advection is ~1.8 times that in summer [*Whelpdale et al.*, 1984] and the biosphere less active, export of pollution via this major outflow pathway is likely a significant source of anthropogenic CO_2 to the region.

4. Summary

[36] High-precision airborne measurements of atmospheric CO_2 mixing ratios were obtained throughout the troposphere over North America and adjacent oceans during the summer of 2004. The INTEX-NA observations substantially enhance the available base of information on the regional-scale distributions of CO_2 in the free troposphere. Results emphasize the observed concentrations were the result of myriad competing processes occurring, at times, external to North America. Our abilities to forecast climate change are reliant on an understanding of the underlying processes such as those revealed by the INTEX-NA data set.

[37] **Acknowledgments.** We gratefully acknowledge the outstanding contributions from Charlie Hudgins, Sandy Branham, Jim Plant, Ali Aknan, and John Barrick during INTEX-NA. We would like to thank Ronald Cohen and Qing Liang for the use of their data and two anonymous reviewers for their insightful comments. We also thank the DC-8 crew and staff for their helpful mission support. This research was supported by the NASA Tropospheric Chemistry Program.

References

Alexeyev, V. A., and R. A. Birdsey (1998), *Carbon storage in forests and peatlands of Russia*, U. S. D. A. Forest Service Northeastern Research Station, Randor.

Amiro, B. D., et al. (2001), Direct carbon emissions from Canadian forest fires, 1959 to 1999, *Can. J. Res.*

Anderson, B. E., et al. (1996), Airborne observations of spatial and temporal variability of tropospheric carbon dioxide, *J. Geophys. Res.*, *101*, 1985–1997.

Andreae, M. O., and P. Merlet (2001), Emission of trace gases and aerosols from biomass burning, *Global Biogeochem. Cycles*, *15*, 955–966.

Andreae, M. O., et al. (1988), Vertical distribution of dimethylsulfide, sulfur dioxide, aerosol ions, and radon over the northeast Pacific Ocean, *J. Atmos. Chem.*, *6*, 149–173.

Apps, M. J., et al. (1993), Boreal forests and tundra, *Water Air Soil Pollut.*, *70*, 39–53.

Berntsen, T. K., et al. (1999), Influence of Asian emissions on the composition of air reaching the North Western United States, *Geophys. Res. Lett.*, *26*, 2171–2174.

Bertram, T. H., et al. (2007), Direct measurements of the convective recycling of the upper Troposphere, *Science*, *315*, doi:10.1126/science.1134548.

Boering, K. A., et al. (1994), Tracer-tracer relationships and lower stratospheric dynamics: CO2 and N2O correlations during SPADE, *Geophys. Res. Lett.*, *21*, 2567–2570.

Bourgeau-Chavez, L. L., et al. (Eds.) (2000), *Characteristics of lorest ecozones in the North American Boreal Region*, pp. 258–273, Springer-Verlag, New York.

Bousquet, P., et al. (2000), Regional changes in carbon dioxide fluxes of land and oceans since 1980, *Science*, *17*, 1342–1346.

Cahoon, D. R., et al. (1994), Satellite analysis of the severe 1987 forest fires in Northern China and Southern Siberia, *J. Geophys. Res.*, *99*, 18,627–18,638.

Campbell, J. E., et al. (2007), Analysis of anthropogenic CO2 signal in ICARTT using a regional chemical transport model and observed tracers, *Tellus, Ser. A and Ser. B*, *59B*, 199–210.

Chatfield, R. B., and P. J. Crutzen (1984), Sulfur dioxide in remote oceanic air: Cloud transport of reactive precursors, *J. Geophys. Res.*, *89*, 7111–7132.

Chedin, A., et al. (2003), The feasibility of monitoring CO2 from high-resolution infrared sounders, *J. Geophys. Res.*, *108*(D2), 4064, doi:10.1029/2001JD001443.

Chen, J. M., et al. (1999), Extending aircraft- and tower-based CO2 flux measurements to a boreal region using a Landsat thematic mapper land cover map, *J. Geophys. Res.*, *104*, 16,859–16,877.

Conard, S. G., et al. (2002), Determining effects of area burned and fire severity on carbon cycling and emissions in Siberia, *Clim. Change*, *55*, 197–211.

Conway, T. J., et al. (1994), Evidence for interannual variability of the carbon cycle from the National Oceanic and Atmospheric Administration/Climate Monitoring and Diagnostics Laboratory Global Air Sampling Network, *J. Geophys. Res.*, *99*, 22,831–22,855.

Cooper, O. R., et al. (2001), Trace gas signatures of the airstreams within North Atlantic cyclones: Case studies from the North Atlantic Regional Experiment (NARE'97) aircraft intensive, *J. Geophys. Res.*, *106*, 5437–5456.

Crosbie, T. M., et al. (1977), Variability and selection advance for photosynthesis in Iowa stiff stalk synthetic maize population, *Crop Sci.*, *17*, 511–514.

Crutzen, P., and M. Andreae (1990), Biomass burning in the tropics: Impact on atmospheric chemistry and biogeochemical cycles, *Science*, *250*, 1669–1678.

Curtis, P. E., et al. (1969), Varietal effects in soybean photosynthesis and photorespiration, *Crop Sci.*, *9*, 323–327.

Damoah, R., et al. (2006), A case study of pyro-convection using transport model and remote sensing data, *Atmos. Chem. Phys.*, *6*, 173–185.

Dickerson, R. R., et al. (1987), Thunderstorms: An important mechanism in the transport of air pollutions, *Science*, *235*, 460–465.

Dickerson, R. R., et al. (1995), Large scale pollution of the atmosphere over the remote Atlantic Ocean: Evidence from Bermuda, *J. Geophys. Res.*, *100*, 8945–8952.

Dye, J. E., et al. (2000), An overview of the Stratospheric-Tropospheric Experiment Radiation, Aerosols, and Ozone (STERAO)-Deep convection experiment with results for the July 10, 1996 storm, *J. Geophys. Res.*, *105*, 10,023–10,046.

Ehleringer, J., and R. W. Pearcy (1983), Variation in quantum yield for CO2 uptake among C3 and C4 plants, *Plant Physiol.*, *73*, 555–559.

EPA, U. S. (2006), *Inventory of U. S. greenhouse gas emission and sinks: 1990–2004*, edited by U. S. E. P. Agency, pp. EPA 430-R-406-002.

Fan, S., et al. (1998), A large terrestrial carbon sink in North America implied by atmospheric and oceanic carbon dioxide data and models, *Science*, *282*, 442–446.

Fehsenfeld, F. C., et al. (1996), Transport and processing of O3 and O3 precursors over the North Atlantic: An overview of the 1993 North Atlantic Regional Experiment (NARE) summer intensive, *J. Geophys. Res.*, *101*, 28,877–28,891.

French, N. H. F., et al. (Eds.) (2000), *Carbon release from fires in the North American boreal forest*, Springer Verlag, New York.

French, N. H. F., et al. (2003), Variability in the emission of carbon-based trace gases from wildfire in the Alaskan boreal forest, *J. Geophys. Res.*, *108*(D1), 8151, doi:10.1029/2001JD000480.

Fuelberg, H. E., et al. (2007), Meteorological conditions and anomalies during INTEX-NA, *J. Geophys. Res.*, doi:10.1029/2006JD007734, in press.

Fung, I. Y., et al. (2005), Evolution of carbon sinks in a changing climate, *PNAS*, *102*, 11,201–11,206.

Goodale, C. L., et al. (2001), Forest carbon sinks in the northern hemisphere, *Ecol. Appl.*, *12*, 891–899.

Gurney, K. R., et al. (2002), Towards robust regional estimates of CO2 sources and sinks using atmospheric transport models, *Nature*, *415*, 626–630.

Gurney, K. R., et al. (2004), Transcom 3 inversion intercomparison: Model mean results for the estimation of seasonal carbon sources and sinks, *Global Biogeochem. Cycles*, *18*, GB1010, doi:10.1029/2003GB002111.

Hall, T. M., and M. J. Prather (1993), Simulations of the trend and annual cycle in stratospheric CO2, *J. Geophys. Res.*, *98*, 10,573–10,581.
Hauf, T., et al. (1995), Rapid vertical transport by an isolated midlatitude thunderstorm, *J. Geophys. Res.*, *100*, 22,957–22,970.
Holland, E. A., et al. (1997), Variations in the predicted spatial distribution of atmospheric nitrogen deposition and their impact on carbon uptake by terrestrial ecosytems, *J. Geophys. Res.*, *102*, 15,849–15,866.
Hudson, R. J. M., et al. (1994), Modeling the global carbon cycle: Nitrogen fertilization of the terrestrial biosphere and the missing CO2 sink, *Global Biogeochem. Cycles*, *8*, 307–334.
Huntrieser, H., et al. (2002), Airborne measurements of NOx, tracer species, and small particles during the European lightning nitrogen oxides experiment, *J. Geophys. Res.*, *107*(D11), 4113, doi:10.1029/2000JD000209.
IPCC (2001), *Climate Change*, Cambridge University Press, Cambridge, United Kingdom and New York, NY.
IPCC (2007), Climate change 2007: The physical science basis, intergovernmental panel on climate change.
Jacob, D. J., et al. (1999), Effect of rising Asian emissions on surface ozone in the United States, *Geophys. Res. Lett.*, *26*, 2175–2178.
Jacob, D. J., et al. (2003), Transport and Chemical Evolution over the Pacific (TRACE-P) aircraft mission: Design, execution, and first results, *J. Geophys. Res.*, *108*(D20), 9000, doi:10.1029/2002JD003276.
Jaffe, D. A., et al. (2003), Six new episodes of trans-Pacific transport of air pollutants, *Atmos. Environ.*, *37*, 391–404.
Kaminski, T., et al. (1999), A coarse grid three-dimensional global inverse model of the atmospheric transport 2. Inversion of the transport of CO2 in the 1980s, *J. Geophys. Res.*, *104*, 18,555–18,582.
Kasischke, E. S., and L. A. Bruhwiler (2002), Emissions of carbon dioxide, carbon monoxide and methane from boreal forest fires in 1998, *J. Geophys. Res.*, *108*(D1), 8146, doi:10.1029/2001JD000461.
Kasischke, E. S., and J. F. Johnstone (2005), Variation in postfire organic layer thickness in a black spruce forest complex in interior Alaska and its effects onslil temperature and moisture, *Can. J. For. Res.*, *35*, 2164–2177.
Kheshgi, H. S., et al. (1996), Accounting for the missing carbon-sink with the CO2 fertilization effect, *Clim. Change*, *33*, 31–62.
Korontzi, S., et al. (2003), Seasonal variation and ecosystem dependence of emission factors for selected trace gases and PM2.5 for southern African Savanna fires, *J. Geophys. Res.*, *108*(D24), 4578, doi:10.1029/2003JD003730.
Krakauer, N., et al. (2005), Compatibility of surface and aircraft station networks for inferring carbon fluxes, paper presented at TransCom Meeting, Paris, France.
Kritz, M. A., et al. (1990), the China Clipper: Fast advective transport of radon-rich air from the Asian boundary layer to the upper troposphere near California, *Tellus, Ser. A and Ser B.*, *4213*, 46–61.
Li, Q., et al. (2005), North American pollution outflow and the trapping of convectively lifted pollution by upper-level anticyclone, *J. Geophys. Res.*, *110*, D10301, doi:10.1029/2004JD005039.
Liang, Q., et al. (2007), Summertime influence of Asian pollution in the free troposphere over North America, *J. Geophys. Res.*, *112*, D12S11, doi:10.1029/2006JD007919.
Liousse, C., et al. (1996), A global three-dimensional model study of carbonaceous aerosols, *J. Geophys. Res.*, *101*, 19,411–19,432.
Logan, J. A., et al. (1981), Tropospheric chemistry: A global perspective, *J. Geophys. Res.*, *86*, 7210–7254.
MacDonald, R. C., and R. Fall (1993), Detection of substantial emissions of methanol from plants to the atmosphere, *Atmos. Environ.*, *27A*, 1709–1713.
Merrill, J. T., and J. L. Moody (1996), Synoptic meteorology and transport during the North Atlantic Regional Experiment (NARE) intensive: Overview, *J. Geophys. Res.*, *101*, 28,903–28,921.
Millet, D. B., et al. (2006), Chemical characteristics of North American surface-layer outflow: Insights from Chebogue point, Nova Scotia, *J. Geophys. Res.*, *111*, D23S53, doi:10.1029/2006JD007287.
Milne, P. J., et al. (2000), Nonmethane hydrocarbon mixing ratios in continental outflow air from eastern North America: Export of ozone precursors to Bermuda, *J. Geophys. Res.*, *105*, 9981–9990.
Moody, J. L., et al. (1996), Meteorological mechanisms for transporting O3 over the western North Atlantic Ocean: A case study for August 24–29, 1993, *J. Geophys. Res.*, *101*, 29,213–29,227.
Mullendore, G. L., et al. (2005), Cross-tropopause tracer transport in midlatitude convection, *J. Geophys. Res.*, *110*, D06113, doi:10.1029/2004JD005059.
Myneni, R. B., et al. (2001), A large carbon sink in the woody biomass of Northern forests, *PNAS*, *98*, 14,784–14,789.
Nakazawa, T. K., et al. (1991), Temporal and spatial variations of upper tropospheric and lower stratospheric carbon dioxide, *Tellus, Ser. A. and Ser. B*, *43B*, 106–117.
Nemani, R. R., et al. (2003), Climate-driven increases in global terrestrial net primary production from 1982 to 1999, *Science*, *300*, 1560–1563.
Nowak, J. B., et al. (2004), Gas-phase chemical characteristics of Asian emission plumes observed during ITCT 2K2 over the eastern North Pacific Ocean, *J. Geophys. Res.*, *109*, D23519, doi:10.1029/2003JD004488.
O'Neill, K. P. (2000), *Changes in carbon dynamics following wildfire in soils of interior Alaska*, Duke University, Durham, N. C.
O'Neill, K. P., et al. (2002), Seasonal and decadal patterns of soil carbon uptake and emission along an age-sequence of burned black spruce stands in interior Alaska, *J. Geophys. Res.*, *107*(D1), 8155, doi:10.1029/2001JD000443.
Palmer, P. I., et al. (2006), Using CO2:CO correlations to improve inverse analyses of carbon fluxes, *J. Geophys. Res.*, *111*, D12318, doi:10.1029/2005JD006697.
Parrish, D. D., et al. (1992), Indications of photochemical histories of Pacific air masses from measurements of atmospheric trace species at Pt. Arena, California, *J. Geophys. Res.*, *97*, 15,883–15,901.
Parrish, D. D., et al. (2004), Intercontinental Transport and Chemical Transformation 2002 (ITCT 2K2) and Pacific Exploration of Asian Continental Emission (PEACE) experiments: An overview of the 2002 winter and spring intensives, *J. Geophys. Res.*, *109*, D23501, doi:10.1029/2004JD004980.
Pfister, G., et al. (2005), Quantifying CO emissions from the 2004 Alaskan wildfires suing MOPITT CO data, *Geophys. Res. Lett.*, *32*, L11809, doi:10.1029/2005GL022995.
Pickering, K. E., et al. (1988), Trace gas transport in the vicinity of frontal convective clouds, *J. Geophys. Res.*, *93*, 759–773.
Prueger, J. H., et al. (2004), Carbon dioxide dynamics during a growing season in midwestern cropping systems, *Environ. Manage.*, *33*, s330–s343.
Ray, E. A., et al. (1999), Transport into the Northern Hemisphere lower-most stratosphere revealed by in situ tracer measurements, *J. Geophys. Res.*, *104*, 26,565–26,580.
Richter, C., et al. (Eds.) (2000), *Postfire stimulation of microbial decomposition in black spruce (Picea mariana L.) forest soils*, Springer-Verlag, New York.
Rodenbeck, C., et al. (2003), CO2 flux history 1982–2001 inferred from atmospheric data using a global inversion of atmospheric transport, *Atmos. Chem. Phys.*, *3*, 1919–1964.
Schade, G. W., and A. H. Goldstein (2006), Seasonal measurements of acetone and methanol: Abundances and implications for atmospheric budgets, *Global Biogeochem. Cycles*, *20*, GB1011, doi:10.1029/2005GB002566.
Schindler, D. W., and S. E. Bayley (1993), The biosphere as an increasing sink for atmospheric carbon - Estimates from increased nitrogen deposition, *Global Biogeochem. Cycles*, *7*, 717–733.
Seiler, W., and P. J. Crutzen (1980), Estimates of gross and net fluxes of carbon between the biosphere and the atmosphere from biomass burning, *Clim. Change*, *2*, 387–395.
Siegenthaler, U., et al. (2005), Stable carcon cycle-Climate relationship during the late pleistocene, *Science*, *310*, doi:10.1126/science.1120130.
Singh, H. B., et al. (2000), Distribution and fate of selected oxygenated organic species in the troposphere and lower stratosphere over the Atlantic, *J. Geophys. Res.*, *105*, 3795–3806.
Singh, H. B., et al. (2006), Overview of the summer 2004 Intercontinental Chemical Transport Experiment-North America (INTEX-A), *J. Geophys. Res.*, *111*, D24S01, doi:10.1029/2006JD007905.
Sinha, P., et al. (2003), Emissions of trace gases and particles from savanna fires in southern Africa, *J. Geophys. Res.*, *108*(D13), 8487, doi:10.1029/2002JD002325.
Soja, A. J., et al. (2004), Estimating fire emissions and disparities in boreal Siberia (1998–2002), *J. Geophys. Res.*, *109*, D14S06, doi:10.1029/2004JD004570.
Stephens, B. B., et al. (2007), Weak northern and strong tropical land carbon ptake from vertical profiles of atmospheric CO2, *Science*, *316*, 1732–1735.
Stocks, B. J., et al. (1998), Climate change and forest fire potential in Russian and Canadian boreal forests, *Clim. Change*, *38*, 1–13.
Stohl, A., and T. Trickl (1999), A textbook example of long-range transport: Simultaneous observation of ozone maxima of stratospheric and North American origin in the free troposphere over Europe, *J. Geophys. Res.*, *104*, 30,445–30,462.
Thompson, A. M., et al. (2007), IONS-04 (INTEX Ozonesonde Network Study, 2004): PerspectIve on summertime UT/LS (Upper Troposphere/Lower Stratosphere) ozone over northeastern North America, *J. Geophys. Res.*, *112*, D12S12, doi:10.1029/2006JD007441.
Tiwari, Y. K., et al. (2006), Comparing CO2 retrived from atmospheric infrared sounder with model predictions: Implications for constraining

surface fluxes and lower-to-upper troposphere transport, *J. Geophys. Res.*, *111*, D17106, doi:10.1029/2005JD006681.
Townsend, A. R., et al. (1996), Spatial and temporal patterns in terrestrial carbon storage due to deposition of fossil fuel nitrogen, *Ecol. Appl.*, *6*, 806–814.
Turetsky, M. R., et al. (2004), Historical burn area in western Canadian peatlands and its relationship to fire weather indices, *Global Biogeochem. Cycles*, *18*, GB4014, doi:10.1029/2004GB002222.
Turner, D. P., et al. (1995), A carbon budget for forests of the conterminous United States, *Ecol. Appl.*, *5*, 421–436.
Turquety, S., et al. (2007), Inventory of boreal fire emissions for North America in 2004: The importance of peat burning and pyro-convective injection, *J. Geophys. Res.*, *112*, D12503, doi:10.1029/2006JD007281.
Vay, S. A., et al. (1999), Airborne observations of the tropospheric CO2 distribution and its controlling factors over the South Pacific Basin, *J. Geophys. Res.*, *104*, 5663–5676.
Vay, S. A., et al. (2003), Influence of regional-scale anthropogenic emissions on CO2 distributions over the western North Pacific, *J. Geophys. Res.*, *108*(D20), 8801, doi:10.1029/2002JD003094.
Wang, J.-W., et al. (2007), Observations and simulations of synoptic, regional, and local variations in atmospheric CO2, *J. Geophys. Res.*, *112*, D04108, doi:10.1029/2006JD007410.
Ward, D. E., et al. (1996), Effect of fuel composition on combustion efficiency and emission factors for African savanna ecosystems, *J. Geophys. Res.*, *101*, 23,569–23,576.
Washenfelder, R. A., et al. (2006), Carbon dioxide colomn abundances at the Wisconsin Tall Tower site, *J. Geophys. Res.*, *111*, D22305, doi:10.1029/2006JD007154.
Whelpdale, D. M., et al. (1984), Advection climatology for the east coast of North America, *Atmos. Environ.*, *18*, 1311–1327.
Yang, Z. H., et al. (2002), Atmospheric CO2 retrived from ground-based near IR solar spectra, *Geophys. Res. Lett.*, *29*(9), 1339, doi:10.1029/2001GL014537.
Yienger, J. J., et al. (2000), The episodic nature of air pollution transport from Asia to North America, *J. Geophys. Res.*, *105*, 26,931–26,945.
Yokelson, R. J., et al. (1999), Emissions of formaldehyde, acetic acid, methanol, and other trace gases from biomass fires in North Carolina measured by airborne Fourier transform infrared spectroscopy, *J. Geophys. Res.*, *104*, 30,109–30,125.
Zoltai, S. C., and P. J. Martikainen (Eds.) (1996), *Postfire stimulation of microbial decomposition in black spruce (Picea mariana L.) forest soils*, Springer-Verlag, New York.

M. A. Avery, G. S. Diskin, G. W. Sachse, and S. A. Vay, NASA Langley Research Center, Hampton, VA 23681, USA.
D. R. Blake and N. J. Blake, Department of Chemistry, University of California, Irvine, CA 92697, USA.
Y. Choi and A. J. Soja, NASA Langley Research Center, National Institute of Aerospace, 100 Exploration Way, Hampton, VA 23666, USA. (ychoi@nianet.org)
A. Fried, National Center for Atmospheric Research, Boulder, CO 80307, USA.
H. E. Fuelberg, Department of Meteorology, Florida State University, Tallahassee, FL 32306, USA.
S. R. Nolf, Computer Sciences Corporation, Hampton, VA 23666, USA.
L. Pfister and H. B. Singh, NASA Ames Research Center, Moffett Field, CA 94035, USA.
K. P. Vadrevu, Agroecosystem Management Program, Ohio Agricultural Research and Development Center (OARDC), The Ohio State University, Wooster, OH 44691, USA.
J.-H. Woo, Department of Advanced Technology Fusion, Konkuk University, Seoul, Korea.